NATIONAL ADVISORY COMMITTEE FOR AERONAUTICS

TECHNICAL MEMORANDUM

No. 1118

THE FLOW THROUGH AXIAL TURBINE STAGES OF LARGE RADIAL BLADE LENGTH

By Eckert and Korbacher

Institute for Engine Research
Hermann Göring Aeronautical Research Foundation
Braunschweig, Germany

Washington
April 1947

NATIONAL ADVISORY COMMITTEE FOR AERONAUTICS

TECHNICAL MEMORANDUM NO. 1118

THE FLOW THROUGH AXIAL TURBINE STAGES OF LARGE RADIAL BLADE LENGTH*

By Eckert and Korbacher

I. INTRODUCTION

The blades of the last stages of steam turbines generally have great radial length, to the extent that the outside diameter of the blading is as much as twice the inside diameter. Likewise with gas turbines, it is desirable to select a large ratio of outside-to-inside diameters in order to achieve small turbine dimensions. It is principally this outside diameter that determines the dimensions; and for a given required gas-flow velocity, this diameter will be inversely proportional to the degree to which the area corresponding to it is utilized for gas flow, that is, it will decrease with a decrease in the relative inside diameter. The relations are similar for axial superchargers.

In such bladings of relatively great length, the flow through the blades is markedly different at different points along the blade length. Namely, wherever a twist occurs in the flow line, centrifugal forces influence the portions of gas moving in curved paths. The result of this is an increase of pressure from inner to outer portions of the annular space between inner and outer circumferences. The pressure drop occurring in a turbine stage is thus divided differently between the stator and rotor toward the hub than toward the outer circumference. This phenomenon is of great importance in the design of the blading and must be considered in determining the form of the blades, if good efficiency is to be obtained. Amazingly enough, it has been treated very little in the literature. A. Stodola in the fourth edition of his classic book on turbine construction (reference 1) briefly discusses the matter and makes some estimates of the order of magnitude of pressure increase in a radial direction. However, this section is omitted in the later editions. Subsequently,

---

*"Die Strömung durch Axialturbinen-Stufen von großer Schaufelhöhe." Deutsche Luftfahrtforschung, Forschungsbericht Nr. 1750. Luftfahrtforschungsanstalt Hermann Göring, Braunschweig, Inst. f. Motorenforschung, ZWB, Feb. 18, 1943, pp. 1-39.

G. Darrieus (reference 2) studied the same phenomenon and attempted to clarify it in terms of the aerofoil theory of Prandtl. However, he only qualitatively discussed the phenomenon. A calculation of the flow and pressure relations has, to the best of our knowledge, not been undertaken. Quite recently W. Hartmann (reference 3) measured the difference in pressure between the inner and outer walls behind a turbine stator. The results showed a somewhat smaller difference than that obtained by calculation for a flow that is in accordance with the spiral formula $c_u r$ = constant (c_u = peripheral component of the velocity; r = radius). Hartmann refers to the difficulties in making an exact measurement of pressures in the annular space defined by a turbine blading and consequently necessary inaccuracies in the measurements obtained. In this paper a calculation of the flow in turbine blading will be reported that will include the calculation of the effect of centrifugal force. In connection therewith a negligible viscosity of the flowing gas and a flow of rotational symmetry will be postulated, that is, the same assumptions that are made by the Euler turbine theory, which is in general use for turbine calculations. As in the Euler formulas, the frictional losses on the stator and rotor blades will be allowed for subsequently through the velocity coefficients φ for the stator and ψ for the rotor. The calculation was made by the first author (Eckert) a few months ago. Since then the experiments of the second author (Korbacher) with a test rig of his own design have satisfactorily confirmed the results for the stator. Therefore the mathematical method can now be published together with the experimental results obtained so far[1].

II. CALCULATION OF THE FLOW BEHIND THE STATOR

1. Twisted Blades

The flow as found behind a stator alone will first be investigated. That is, the respective rotor is to be thought of as not yet put in place. Figure 1 schematically presents an axial section through such a stator. The stator blades occupy the annular space between the inner diameter D_i and the outer diameter D_a. A system of polar coordinates so placed in the stator that z falls along the axis of the turbine, r is the distance from the axis of rotation, and ϵ is the angle must be imagined. The stator blades are understood to be so close together that the small velocity variations across the blade spacing can be neglected and the flow regarded as axially symmetrical, that is,

---

[1]We owe thanks to Professor C. Pfleiderer, Doctor of Engineering, for various suggestions to our work.

independent of ϵ. The flow is assumed to approach the stator in a strictly axial direction with a velocity c_{m0} which is uniform over the whole cross section of the annular space. In other words, the whirl component of the velocity is zero in front of the stator. A twist is then given to the flow by the stator blades. In the plane 1-1 close behind the stator, which is to be the site of the following investigation of velocity relations, let c_1, which has the components c_{m1}, c_{u1}, and c_{r1}, represent the velocity at the distance r from the axis. Owing to the whirl component c_{u1} of the velocity, centrifugal forces operate upon the particles of fluid and effect an increase of the pressure p_1 in a radial direction. Observe a portion of fluid at a distance r from the axis of rotation, with base area df and height dr. Its volume is thus $df\,dr$ and its mass $\frac{\gamma}{g} df\,dr$ (γ = specific weight; g = acceleration of gravity). Upon this portion of gas there operates in a radial direction the centrifugal force $\frac{\gamma}{g}\frac{c_{u1}^2}{r} df\,dr$, also a pressure force of the magnitude $df\frac{\partial p_1}{\partial r}dr$ [NACA comment: The German did not distinguish between partial and total derivatives. In order to avoid confusion partial derivatives have been distinguished from total derivatives.], and an inertia force $\frac{\gamma}{g} df\,dr\frac{dc_{r1}}{dt}$. Because c_r may be a function of z and r, the following applies to steady flow

$$\frac{dc_{r1}}{dt} = \frac{\partial c_{r1}}{\partial r}\frac{dr}{dt} + \frac{\partial c_{r1}}{\partial z}\frac{dz}{dt} = c_{r1}\frac{\partial c_{r1}}{\partial r} + c_{m1}\frac{\partial c_{r1}}{\partial z}$$

By equating the three forces the following equation is obtained

$$\frac{c_{u1}^2}{r} - \frac{dc_{r1}}{dt} = \frac{g}{\gamma}\frac{dp_1}{dr}$$

Note that during the flow through the blading, the inertia force acquires considerable magnitude, especially when the dimension of the blade-row in z direction is small. This can be seen from the course of the flow lines through the stator, as shown in figure 3. At the point of exit from the blading, the radial velocities have nevertheless already decreased greatly, therefore in the plane 1-1, which is but little removed from the blade-exit plane, they may already be ignored. This appears from the measurements to be reported subsequently. If the radial velocity c_{r1} in the plane 1-1 is set equal to zero, for the preceding equation the following simpler form is obtained

$$\frac{c_{u1}^2}{r} = \frac{g}{\gamma}\frac{dp_1}{dr} \tag{1}$$

From it the radial increase in pressure can be calculated as soon as the magnitude of the whirl component c_{u1} as a function of r is known. With the close spacing assumed for the blades, the direction of the velocity vector c is at once known, because at a short distance behind the stator blades it will be equal to the exit angle of the blades α_1. If this angle α_1 is measured with respect to the peripheral direction, the following relation for the whirl component c_u is obtained

$$c_1 = \frac{c_{u1}}{\cos \alpha_1} \tag{2}$$

in which the angle α_1 is to be regarded as a function of r determined by the blade form. Outside the boundary layers at the blade surfaces, which become infinitely thin at negligible viscosity of the flowing gas, the flow may be regarded as frictionless. The following Bernoulli equation then applies along a flow line through the stator

$$\int \frac{dp}{\gamma} + \frac{c^2}{2g} = K \tag{3}$$

At small flow velocities the integral is replaced by the expression $\frac{p}{\gamma}$. The constant K is then simply the total pressure divided by the weight density γ. At large velocities, γ may no longer be regarded as constant. The integral $\int \frac{dp}{\gamma}$ is then suitably taken for the given pressure p from a Mollier i-s diagram. It is the same as the enthalpy i (heat content) in mechanical units (mkg/kg). The Bernoulli constant is then the enthalpy corresponding to the impact pressure. In the general case, when no potential flow is involved, it has a different value for each flow line. Mathematically formulated this means that K in the cross section 1-1 may be a function of r. But in the present case it may easily be shown that K has the same numerical value for all flow lines. Because the velocity c in front of the stator is unvarying throughout the radial length of the blades and because the flow is free of twist at that point and is therefore of uniform pressure over the cross section, equation (3) gives the same value of the constant for every flow line. The total pressure is therefore uniform over the whole flow field. If equation (3) is now differentiated with respect to r

$$\frac{1}{\gamma}\frac{dp}{dr} + \frac{c}{g}\frac{dc}{dr} = 0 \tag{4}$$

By applying the equation to the cross section 1-1 and eliminating the pressure by means of equation (1)

$$\frac{c_{ul}^2}{r} = -c_1 \frac{dc_1}{dr} \tag{5}$$

In order to substitute its peripheral component for velocity c_1 in equation (5), equation (2) is differentiated with respect to r

$$\frac{dc_1}{dr} = \frac{1}{\cos \alpha_1}\frac{dc_{ul}}{dr} + \frac{c_{ul} \sin \alpha_1}{\cos^2 \alpha_1}\frac{d\alpha_1}{dr} \tag{6}$$

Thereby equation (5) becomes

$$\frac{c_{ul}}{r} = -\frac{1}{\cos^2 \alpha_1}\frac{dc_{ul}}{dr} - \frac{c_{ul} \tan \alpha_1}{\cos^2 \alpha_1}\frac{d\alpha_1}{dr} \tag{7}$$

or

$$\frac{dc_{ul}}{c_{ul}} = -\left(\frac{\cos^2 \alpha_1}{r} + \tan \alpha_1 \frac{d\alpha_1}{dr}\right)dr = -f(r)dr \tag{8}$$

The expression in parentheses is a function $f(r)$ of r, determined by the blade twist. The differential equation when solved gives

$$\ln c_{ul} = -\int f(r)dr + \text{constant}$$

or if $\ln a_1$ [NACA comment: The quantities a and a_1 appear to be the same.] is substituted for the constant,

$$c_{ul} = a_1 e^{-\int f(r)dr} \tag{9}$$

The constant a_1 is to be determined from the quantity of flow. This will be further discussed.

2. Nontwisted Blades

If the stator has nontwisted blades, the angle α_1 is then independent of r, and from equation (8) is obtained

$$\frac{dc_{ul}}{c_{ul}} = - \cos^2 \alpha_1 \frac{dr}{r} \tag{10}$$

By integration of this equation

$$c_{ul}\, r^{\cos^2 \alpha_1} = \text{constant} = a_1 \tag{11}$$

The axial component of the velocity is determined from $c_{ml} = c_{ul} \tan \alpha_1$

$$c_{ml}\, r^{\cos^2 \alpha_1} = a_1 \tan \alpha_1 = \text{constant} \tag{12}$$

The constant a_1 is obtained from the weight of gas passing through the stator in a unit of time, which is represented by G. The equation is

$$G = \int_{r_i}^{r_a} \gamma\, c_{ml}\, 2r\pi\, dr$$

Because of the dependence of the specific weight γ upon the pressure, an exact evaluation of the equation is very difficult. If a mean value γ_m is used, from equation (12) the following expression for a_1 is obtained

$$a_1 = \frac{G}{\gamma_m} \frac{1 + \sin^2 \alpha_1}{2\pi \tan \alpha_1 \left(r_a^{\sin^2 \alpha_1 + 1} - r_i^{\sin^2 \alpha_1 + 1} \right)} \tag{13}$$

If the annular space occupied by the stator blading is cylindrical, as in figure 1, then a_1 can also be expressed in terms of c_{m0}, the velocity ahead of the stator. At this latter point the following equation applied

$$G = \gamma_0\, c_{m0}\, \pi\, (r_a^2 - r_i^2)$$

Thus is obtained

$$a_1 = \frac{\gamma_0}{\gamma_m} c_{m0} \frac{(1 + \sin^2 \alpha_1)(r_a^2 - r_i^2)}{2 \tan \alpha_1 \left(r_a^{\sin^2 \alpha_1 + 1} - r_i^{\sin^2 \alpha_1 + 1} \right)} \tag{14}$$

The curve of pressure over the cross section 1-1 is obtained from equation (3). If the velocity at the inner diameter is represented as c_{i1}, then

$$\int_{r_i}^{r} \frac{dp_1}{\gamma} = \frac{1}{2g} (c_{i1}^2 - c_1^2) \tag{15}$$

and, taking account of equations (2) and (11),

$$\int_{r_i}^{r} \frac{dp_1}{\gamma} = \frac{1}{2g} c_{i1}^2 \left[1 - \left(\frac{r_i}{r} \right)^2 \cos^2 \alpha_1 \right] \tag{16}$$

The quantity $\int_{r_i}^{r} \frac{dp}{\gamma}$ represents simply the negative value of the heat drop between the respective radii in question. From it with the aid of the entropy diagram, the pressure difference Δp can at once be taken. At small flow velocities $\int_{r_i}^{r} \frac{dp}{\gamma} = \frac{\Delta p}{\gamma}$. Equations (11), (12), and (16) are numerically evaluated in figure 2. As only exhibition of the variation of the velocity is considered, the axial velocity at the inner diameter c_{mi1} is set equal to 1. The calculation has been carried out for two blade-exit angles, 30° and 45°. The dashed curve will be discussed later. Behind the stator the axial component is no longer uniform throughout the length of the blades. It is greatest at the inner diameter and decreases toward the outer diameter, that is, the flow is deflected toward the axis of rotation by the stator. The course of the flow lines in passing through a stator with nontwisted blades of 30° exit angle is shown in figure 3. The course shown for the flow lines within the blading is estimated.

3. Irrotational Spiral Flow

With twisted blades it is possible, by appropriate choice of blade-exit angle, to achieve uniformity of the velocity component c_m throughout the length of blade behind the stator as well as ahead of it. In this case it follows from the Bernoulli equation that

$$\int \frac{dp}{\gamma} + \frac{c_u^2}{2g} = K \tag{17}$$

By application of the equation to section 1-1, and by differentiation

$$\frac{g}{\gamma}\frac{dp_1}{dr} + c_{ul}\frac{dc_{ul}}{dr} = 0 \tag{18}$$

By combining this equation with equation (1)

$$\frac{c_{ul}^2}{r} = -c_{ul}\frac{dc_{ul}}{dr} \tag{19}$$

and by integration

$$c_{ul}r = \text{constant} \tag{20}$$

Thus the well-known fact is arrived at that the flow must obey the spiral formula if the axial component c_m is not to vary with the radius after the flow passes through the stator. The range of pressure is given as before by the equation

$$\int_{r_i}^{r}\frac{dp}{\gamma} = \frac{1}{2g}c_{il}^2\cos^2\alpha_i\left[1-\left(\frac{r_1}{r}\right)^2\right]$$

The nontwisted blading produces, as is seen from equation (16) and the above relation, a greater pressure increase than the spiral flow $c_u r = \text{constant}$, if in both cases the angle α_1 and the velocity c_1 are the same. If the two flows are postulated as having the same angle and the same velocity at the center of blade height, then the blading, twisted to produce a flow in accord with the spiral formula, produces a somewhat greater pressure increase. From equation (20) may be determined the variation of blade angle along the blade length that will be necessary to produce the desired flow. As is known, the flow according to equation (20) is vortex-free. However, this does not apply for a spiral flow produced by nontwisted blades or blades with an arbitrarily selected twist. Now the nature of the vortices in the flow will be investigated more exactly.

4. Distribution of Vorticity in the Flow

In a flow subject to vortices a vortex vector W at any point may be defined by the equation

$$W = \text{rotation } \overline{c} \tag{21}$$

The vector is here designated by the mean line. One half the value of this vorticity gives the angular velocity with which the neighboring fluid particles revolve about the vector direction as an axis. The calculation of the vortex strength W can be made with the aid of the Stokes theorem. This theorem states that every component of the vorticity is equal to the circulation $d\Gamma$ around a small surface element standing perpendicular to the direction of the vector component, divided by the magnitude of this surface element df, that is

$$W = \frac{d\Gamma}{df} \tag{22}$$

With the aid of this theorem the three components of the vorticity will be determined. In order to calculate the component in the peripheral direction W_u, the circulation, that is, the line integral of the velocity around a small surface element having sides of length dr and dz (fig. 1) must be developed. At a distance r from the axis of rotation, the axial velocity c_{ml} exists. The line integral along the linear element dz has therefore at this point the value $c_{ml}\,dz$. At the distance r + dr the axial velocity is $c_{ml} + \frac{dc_{ml}}{dr}dr$. At this second point the line integral along dz therefore has the value $\left(c_{ml} + \frac{dc_{ml}}{dr}dr\right)dz$. Along the linear element dr the line integral is zero, because the radial velocity c_r is ignored. As the sum of all the line integrals pertaining to circulation around the surface element, is thus obtained the expression for circulation

$$d\Gamma_{ul} = -\frac{dc_{ml}}{dr}\,dr\,dz$$

and when dividing by the surface area, the following expression for the tangential component of the vortex strength

$$W_{ul} = -\frac{dc_{ml}}{dr} \tag{23}$$

The axial velocity c_{ml} is given by the relation $c_{ml} = c_{ul} \tan \alpha_1$. Thus equation (23) becomes

$$W_{ul} = - \tan \alpha_1 \frac{dc_{ul}}{dr} - \frac{c_{ul}}{\cos^2 \alpha_1} \frac{d\alpha_1}{dr}$$

By substitution of the value of the derivative $\frac{dc_{ul}}{dr}$ from equation (8)

$$W_{ul} = \sin \alpha_1 \cos \alpha_1 \frac{c_{ul}}{r} - c_{ul} \frac{d\alpha_1}{dr} \tag{24}$$

In order to obtain the axial component W_{ml} of the vorticity, the circulation about a surface element with the dimensions dr and $rd\epsilon$ must be developed. The line integral along $rd\epsilon$ at distance r from the axis is $c_{ul}rd\epsilon$. As the distance r increases by dr, the line integral changes by $\frac{d(rc_{ul})}{dr}drd\epsilon$. Because the line integrals along dr are zero, the circulation around the surface element is

$$d\Gamma_{ml} = \frac{d(rc_{ul})}{dr}drd\epsilon$$

The vortex strength obtained by dividing this equation by the surface area is

$$W_{ml} = \frac{1}{r} \frac{d(rc_{ul})}{dr} = \frac{dc_{ul}}{dr} + \frac{c_{ul}}{r} \tag{25}$$

Again eliminating the derivative dc_{ul}/dr by means of equation (8)

$$W_{ml} = \tan \alpha_1 \left(\sin \alpha_1 \cos \alpha_1 \frac{c_{ul}}{r} - c_{ul} \frac{d\alpha_1}{dr} \right) \tag{26}$$

The radial component of the vorticity is zero because of the axial symmetry. Consequently the vector lies in a cylindrical surface (r = constant) and is at an angle δ to the peripheral direction, which is calculated from the equation

$$\tan \delta = \frac{W_{ml}}{W_{ul}}$$

By substituting the expressions for the two vorticity components

$$\delta = \alpha \tag{27}$$

Thus the vortex filaments travel in the current at the exit angle of the stator blading. This result is in agreement with a general hydrodynamic theorem that vortex filaments and current filaments must coincide, if for the flow in question the Bernoulli equation with a fixed value for the constant K applies universally (reference 4). How such vortices come into existence in a current of negligible friction was shown by Prandtl in his explanation of the induced resistance of airfoils.

An airfoil of infinite span in a frictionless current is subject to a force perpendicular to the direction of the free-stream velocity, if into the otherwise vortex-free current a circulation is introduced about the airfoil. The flow around the airfoil is then composed of a circulation-free stream flowing past it plus the circulation flow, which at a greater distance corresponds to the flow field of a potential vortex. Therefore as a first approximation the airfoil can be imagined as replaced by a potential vortex. Such a vortex is subject to the rule that it must either form a continuous circuit or extend to infinity. If the airfoil is of finite span, the vortex with which the airfoil has been replaced must be pictured as being bent rearwards at both ends. See figure 4(a). The true flow relations around the airfoil will be even better represented by considering it as replaced by a whole series of vortices, which bend rearwards at varying distances from the airfoil ends. See figure 4(b). Thus behind the airfoil is obtained a surface of discontinuity, which is entirely composed of adjoining vortex filaments. The distribution of the vortices over the chord of the airfoil is determined by the fact that in every section 1-1 the vortex filaments passing through that cross section will produce just precisely the circulation that exists at this location on the airfoil. A variation in circulation about the airfoil occurring between sections 1-1 and 2-2 corresponds therefore to a definite number of vortex filaments, which leave the rear edge of the airfoil in the area between 1-1 and 2-2. The vortices leaving the airfoil may be very nicely made visible in a water channel by the introduction of air in the vortex axis. Such a flow picture made by H. Drescher of the Aerodynamic Research Institute in Göttingen is reproduced in figure 5. Similar observations were made on marine propellers by Föttinger (reference 5) and on airplane propellers by Betz (reference 6).

The same phenomenon occurs in the stator under investigation whenever the circulation about the individual blade is variable along its length. But this is always the case if the flow produced by the stator is not according to the spiral formula $c_u r = \text{constant}$. This may be seen from figure 6, which shows a developed cylindrical

section through the stator. The circulation about a blade is obtained by developing the line integral along the path 1-2-3-4. The partial integrals for the two paths 1-2 and 3-4 cancel each other by reason of symmetry if these two paths are exactly 1 blade interval apart. Along the line 1-4 the velocity is perpendicular to the path of integration; the line integral there will consequently be zero. There remains only the integral along the line 2-3 and the circulation around a blade therefore has the value $\Gamma_s = c_{u1}a$, if a is the blade interval. The line integral around the circumference is $\Gamma_u = c_u 2r\pi$, or with n blades it is n times the individual blade circulation Γ_s. For a flow in accordance with the spiral formula, the line integral around the circumference is

$$\Gamma_u = c_u 2r\pi = \frac{\text{constant}}{r} 2r\pi = \text{constant}$$

that is, independent of r. Thus the blade circulation is also uniform along the blade length. If on the contrary, the flow does not fulfill the spiral-formula conditions, then the circulation around each blade varies throughout its length. Consequently, a mass of vortex filaments pass from the trailing edge of the blade into the current. This is shown in figure 7. If the blade interval is now reduced more and more, these sheets of vorticity also approach one another more closely and finally as infinitely small blade intervals are reached fill up the entire flow field behind the stator. The progression toward the infinitely small blade intervals, which are necessary to achieve axially symmetrical flow, leads therefore to a flow, uniformly filled with vortices, of the form derived in the previous paragraphs.

III. EXPERIMENTS ON THE STATOR

For the investigation of the spiral flow produced by a stator with nontwisted blading, the test rig shown in figure 8 was designed. The stator occupies the space between the inner tube b of 80-millimeter diameter and the outer tube c of 160-millimeter diameter. The ratio of radii is therefore 2 and the difference of pressure in a radial direction may be expected to be distinctly measurable. In order to obtain a flow through the stator as little disturbed as possible, the air of the room is sucked through the stator by a blower connected to the test rig through a rather long pipe. Special importance was attached to the accurate installation of the stator blades in order to secure a satisfactory axial symmetry of flow. They were set between the inner and outer tubes by a special technique with the aid of a dividing head. The blade section

used is shown in figure 9. The stator consists of 30 blades. The blade-exit angle was optically tested after installation and the variation between blades was within 1 degree. The precision of the blading installation is thus markedly greater than in ordinary turbine construction (reference 3, p. 1). The blade surfaces were polished and the tube walls very carefully processed in order that all surfaces might confidently be regarded as hydraulically smooth. Figure 10 is a photograph of the forward part of the test rig with the stator. In order to avoid disturbance of the flow, the first struts between inner and outer tubes were placed at d at a distance of 195 millimeters downstream from the stator. These struts were of circular section in order to make sure they did not influence the spiral flow. The variation of pressure in the current behind the stator can be measured through a large number of holes e in the inner and outer tubes. In the stream itself the direction of flow is measured by a cylindrical tube of 4-millimeter diameter (reference 7), the static pressure p and total pressure p_g by a small Prandtl pitot tube of 1.5-millimeter diameter and 9.5-millimeter length. As a check on these measurements, the volume of flow and the torque exerted on the stator by the current are also measured. The volume rate of flow may be measured by a diaphragm located at a sufficient distance downstream from the stator behind a straightener that removes the twist from the current. A second possible way of measuring the flow volume is by determining the static pressure ahead of the stator through the hole f. In order to enable measurement of the torque, the stator and the intake portions of the inner and outer tubes are mounted revolvably on the ball bearings g. The two concentric tubes are connected by the stator blades. The break h thus produced in the outer tube is closed by a thin rubber membrane i. This space can be used for pressure measurement, as can the break k in the inner tube.

Measurements with this test rig are still in progress. Of the results so far only those pertaining to a plane 25 millimeters behind the stator will be briefly discussed, in so far as they are applicable to the checking of the calculations set forth. A complete report will be published after the conclusion of the investigation. Figure 11 shows the distribution of static pressure p and total pressure p_g. Within the flow these measurements were carried out with the Prandtl pitot tube. The static pressure at the two walls (at $r/r_1 = 1$ and $r/r_1 = 2$, respectively) is measured through the holes in the walls. From figure 11 it can be seen that the points obtained by the two methods of measurement lie very nicely on one curve. The wall apertures 10 millimeters behind the stator showed within 2 percent of the same pressure difference as

the holes at a distance of 25 millimeters. In the total-pressure readings with the pitot tube, the wake behind the stator blades was still somewhat perceptible. In figure 11 is recorded the minimum value of the pressure drop p_0-p_g, which could be measured with a revolution of the stator. The total pressure ahead of the stator is equal to the pressure p_0 in the air of the room. Because of the flow losses in the stator, this same total pressure is never again quite attained behind the stator. However, the pressure loss p_0-p_g is not great except in the region near the inner tube. It would seem that a breakup of the flow occurs here. This region of greater flow losses increases in breadth with increasing distance from the stator. The corollary may be reasonably deduced that the region is very small immediately behind the stator. With the exception of this region of disturbance and of the immediate neighborhood of the outer wall, the assumption made in the calculations that the total pressure is constant across a section behind the stator agrees in some measure with the actual relations in a fluid subject to friction. The drop p_0-p_g in total pressure as the flow passes through the stator may be taken into account by the introduction of a coefficient φ to modify the theoretical velocity of outflow from the stator. In order to determine the coefficient φ, the measured pressure difference p_a-p_i between outer and inner walls will be compared with that which would be calculated for frictionless flow according to the previous section if the impact pressure of the flow at the inner wall is equal to the pressure drop p_0-p_i at that point. The direction of outflow is determined to be at an angle of 25° to the peripheral direction by means of the cylindrical tube. This direction of flow is also recorded in figure 9. If the theoretical pressure difference p_a-p_i is calculated for this angle of 25° and the ratio of the observed to the calculated pressure difference is found, the numerical value 0.902 is obtained. This must be equal to the square of the coefficient φ. For the coefficient itself the value $\varphi = 0.950$ is thus obtained. A second possible way of determining this is afforded through the measurement of the torque.

The torque measurement in this experiment is 6.25 centimeter kilograms. The corresponding torque for the theoretical flow considered in the previous section may be calculated by means of the following equation

$$Md = \int_{r_i}^{r_a} \gamma \, 2r\pi \, dr \, c_{ml} \frac{r \, c_{ul}}{g}$$

which follows directly from the principle of momentum. After insertion of the exit angle α_1 in this equation and expression of the velocity components in terms of equations (11) and (12), integration gives the expression

$$Md = \pi \frac{\gamma}{g} \frac{\sin (2 \alpha_1)}{2 \sin^2 \alpha_1 + 1} c_{i1}^2 r_i \left[\left(\frac{r_a}{r_i} \right)^{3-2 \cos^2 \alpha_1} - 1 \right]$$

The quantity $\frac{\gamma}{2g} c_{i1}^2$ is simply the dynamic pressure of the flow at the inner wall. If the observed pressure difference p_0-p_i, that is, the dynamic pressure that would be associated with a loss-free drop in the pressure p_i behind the stator is substituted for this, a value of 6.40 centimeter kilograms is obtained for the torque. The difference between the calculated and the observed value may also be explained in terms of the fact that the conversion of pressure into velocity in the stator does not proceed entirely without losses. The stator-velocity coefficient φ may be derived from those quantities also. The square of this coefficient is the ratio of the observed to the calculated torque. For this is obtained the value 0.977. The velocity coefficient itself then comes to 0.988. This value lies within the range established for turbine bladings. Of course, note must be taken in this connection that the coefficient is based on the dynamic pressure at the inner wall, that is, to the maximum velocity. In the next paragraph will be seen why the value calculated from the pressure distribution is lower.

Another basis on which observation may be compared with calculation is to calculate the pressure difference p_a-p_i, which would occur in a frictionless flow having a volume per unit time equal to that of the actually observed flow through the stator. By means of the formulas in the previous section, this is found to be $p_a-p_i = 105.9$ millimeters water or 130.2 millimeters alcohol. From figure 11 the observed pressure difference p_a-p_i was 122 millimeters of alcohol. The calculated pressure difference is thus 6.7 percent greater than the observed. This may be freely explained by the fact that smaller velocities are present at the inner wall due to the greater flow losses and these velocities influence the pressure increase especially strongly because of the markedly curved paths.

Thus the calculated pressure difference between inner and outer walls is found to agree very well with the observed. Likewise the range of static pressure over the annular space between the walls is satisfactorily reflected by the calculation, as a comparison of

figures 2 and 11 shows. The calculations for a gas with negligible friction may thus be applied also to the approximate representation of the relations in a gas subject to friction, if the theoretical speeds are modified by the customary coefficients. In so doing, of course, the losses are considered as distributed equally over the whole length of blade; fine points such as the concentration of the flow losses at the inner wall are naturally not included. The deflection of the current toward the axis, indicated in figure 3, may be made clearly visible by the introduction of a streamer between the blades.

IV. CALCULATION OF FLOW THROUGH THE ROTOR

Now the methods of calculation set forth in section II will be applied to the rotor as well. The section through a turbine stage consisting of rotor and stator is shown in figure 12. The plane of measurement 1-1 lies between stator and rotor. In what follows the velocity and pressure variations in a second plane 2-2 behind the rotor will be set forth. In so doing the assumption will be made that the pressure variations in the plane 1-1 will not be influenced by the rotor. That is, in the following discussion the range of pressures, which were calculated for the stator by itself, will be taken as the basis. This assumption will certainly be correct if the space between stator and rotor is kept sufficiently great, or if the rotor blades have a large axial dimension. But in the case of the small rotor-stator space and small blade widths customary in turbine construction, it remains to be experimentally determined whether the pressure in the space between rotor and stator will be altered as the flow lines are deflected sharply outward, as shown in figure 22. (See reference 9.)[2] Preparations are being made for such measurements on a one-stage turbine with nontwisted stator and rotor blades. In spite of this uncertainty, the following calculations are still of importance for such blade forms, as they provide maximum values for the difference of inflow angles between head and foot of the rotor blades. If the form of the rotor blades is so designed that they will work efficiently in this range of angles of inflow, then the blades will certainly be suitable for the actual flow to be encountered.

---

[2]Measurements by W. Hartmann on a turbine stage (reference 8) appear to indicate that with a narrow rotor-stator space the radial pressure increase in this space is smaller.

In figure 12 the velocity-vector diagrams at entrance to and exit from the rotor are shown. The absolute velocities are designated by c and the relative velocities by w. The rotor velocity at the given radial distance is designated by u. The rotor blades shall be so rounded at the fore edge that throughout the range of inflow angles in question they will permit a flow around the blades without separation. The absolute inflow angles are designated α, the relative angles β. All quantities referring to plane 1-1 are written with the subscript 1 and those relating to plane 2-2 with the subscript 2. The energy drop, which undergoes conversion in the stator, is denoted by h, that converted in the rotor by h'. These drops are obtained from the adiabatic energy drops in the usual manner, deducting the energy losses calculated with the aid of the velocity coefficients φ and ψ. The kinetic energy of the inflow velocity c_0 is also to be included in the total drop H available over the whole stage

$$H = h + h' + \frac{c_0^2}{2g} \tag{28}$$

For the drop in the stator we have

$$h = \frac{1}{2g}(c_1^2 - c_0^2) \tag{29}$$

and correspondingly for the rotor drop

$$h' = \frac{1}{2g}(w_2^2 - w_1^2) \tag{30}$$

Thus the total drop can also be written as

$$H = h' + \frac{c_1^2}{2g} \tag{31}$$

For the following calculations a stator having nontwisted blades will first be assumed. In the final section the general method of calculation will be given, which will also include twisted blades. In general, there also exists a spiral at plane 2-2 and hence a pressure increase toward the outside. Only when the absolute outflow velocity from the rotor has no peripheral component, that is, when it is directed strictly axially, will there by uniform pressure in the plane 2-2. The calculation for this case is also the most simple one.

1. Rotor with Axial Outflow

From the velocity-vector diagram for the rotor inflow, for the relative inflow velocity w_1 is obtained the equation

$$w_1^2 = c_1^2 + u^2 - 2\, c_{u1}\, u \tag{32}$$

For the relative outflow velocity w_2, the equation becomes simpler because the whirl component c_{u2} of the absolute outflow velocity is assumed to be zero.

$$w_2^2 = c_2^2 + u^2 \tag{33}$$

Hence for the rotor drop from equation (30) is obtained the relation

$$h' = \frac{1}{2g}(c_2^2 - c_1^2) + \frac{1}{g}\, c_{u1}\, u \tag{34}$$

Solving for c_2 gives

$$\frac{c_2^2}{2g} = h' + \frac{c_1^2}{2g} - \frac{c_{u1}\, u}{g} \tag{35}$$

or after introduction of the total drop H

$$\frac{c_2^2}{2g} = H - \frac{c_{u1}\, u}{g} \tag{36}$$

By introduction of the values of c_{u1} from equation (11) and of the rotor velocity u from the equation $u = r\omega$ (ω = angular velocity), the following equation is obtained

$$\frac{c_2^2}{2g} = H - \frac{1}{g}\, a_1\, \omega r^{\sin^2 \alpha_1} \tag{37}$$

from which the absolute outflow velocity c_2 from the rotor may be determined.

In figures 13 and 14 the numerical evaluation of this equation for stators with exit angles of 45° and 30°, respectively, is presented. The intake to the stator is here assumed to be strictly axial and of uniform velocity throughout the blade length. The rotor must have

twisted blades so as to give at the rotor speed selected an axial outflow at all points along their length. The leading edge of the blades shall be so designed that no flow separation shall occur (inflow free of shock). This can best be obtained by a rounding-off of the leading edge as shown in figure 12. Because only relative measurements are of importance for the problem in hand, the ratio of radii r/r_1 was chosen as the abscissa. As only relative velocities are of concern, it is assumed that the axial velocity c_{m1} and $c_{m2} = 1$. The rotor speed is so chosen that at the inner radius the pressure p_1 is equal to p_2, that is, at the foot of the blades the rotor operates at equal pressure on both sides. From figures 13 and 14 it can be seen that the axial velocity $c_{m2} = c_2$ behind the rotor decreases in an outward direction in somewhat the same manner as the velocity c_{m1} in front of the rotor.

In the lower halves of these figures is also the degree of reaction R, that is, the ratio of rotor drop h' to total drop H, as well as the work output h_n imparted to the rotor at each point per kilogram of medium flowing through. The latter is obtained from the equation $h_n = \frac{1}{g} c_{u1} u$. It is seen from the graphs that the degree of reaction R rises quite rapidly along the blade from foot to outer end. At 45° and 30° inflow angles the reaction degree reaches 0.5 at radius ratios of 1.9 and 1.6, respectively, that is, the blades operate with 50 percent reaction at those points.

The work output imparted to the rotor likewise increases outwardly along the blade. The Bernoulli equation (3) consequently has behind the rotor a different value for the constant K for each flow line because the withdrawal of energy from each flow line within the rotor is different in amount. Furthermore, it is no longer necessary to fulfill the condition that the vortex filaments coincide with the flow lines. In reality, in the present case the vorticity also stands perpendicular to the direction of flow inasmuch as the axial component of the vorticity W_m (equation (25)) is equal to zero because of the entirely axial outflow velocity. Thus the vortex filaments present in the current in this case run around the axis as closed rings.

In figure 15 is represented the course of the flow lines through a turbine stage. The deflection of the flow toward the axis, which is introduced in the stator, is only to a rather small degree reversed in the rotor.

2. Nontwisted Rotor Blade

If the rotor is equipped with nontwisted blades, it is not possible to achieve axial outflow throughout the length of the blade. Because of the whirl component present in that case, a radial increase of pressure occurs behind the rotor, whereby the calculation is made more difficult. The drop H through the stage is therefore also nonuniform along the blade length. In order to determine it, the drop h' in the rotor is first calculated. For the relative outflow velocity w_2, the following equation applies

$$w_2^2 = c_2^2 + u^2 - 2\, c_{u2}\, u \tag{38}$$

By insertion of the expressions from equations (38) and (32) in equation (30),

$$h' = \frac{1}{2g}\left(c_2^2 - c_1^2\right) + \frac{1}{g}\left(c_{u1}\, u - c_{u2}\, u\right) \tag{39}$$

The drop in the whole stage may now be expressed on the basis of equation (31) as

$$H = \frac{1}{2g}\, c_2^2 + \frac{u}{g}\left(c_{u1} - c_{u2}\right) = -\int \frac{dp}{\gamma} \tag{40}$$

The drop H is again equal to the pressure integral $\int \frac{dp}{\gamma}$. This equation replaces the Bernoulli equation (3). Hence an expression for the radial increase of pressure behind the rotor can also be derived by differentiating with respect to r

$$-\frac{1}{\gamma}\frac{dp_2}{dr} = \frac{1}{2g}\frac{dc_2^2}{dr} + \frac{1}{g}\frac{d}{dr}\left(c_{u1}\, u - c_{u2}\, u\right) \tag{41}$$

A second relation pertaining to the increase of pressure is also to be found in equation (1), which must apply here equally well as an equilibrium of forces. In order to eliminate the velocity c_2 from equation (41), the axial component c_{m2} will be first expressed in terms of the whirl component c_{u2}. From the velocity diagram for the outflow is deduced the equation

$$c_{m2} = \left(u - c_{u2}\right) \tan \beta_2$$

The velocity c_2 is then

$$c_2^2 = \left(u - c_{u2}\right)^2 \tan^2 \beta_2 + c_{u2}^2 \tag{42}$$

By differentiation of this equation with respect to r, it becomes

$$\frac{dc_2^2}{dr} = 2\,(u - c_{u2})\tan^2\beta_2\left(\omega - \frac{dc_{u2}}{dr}\right) + 2\,c_{u2}\,\frac{dc_{u2}}{dr} \qquad (43)$$

By insertion of this relation in equation (41) and elimination of p_2 by means of equation (1), the velocity component c_{u1} by means of equation (11), and the rotor speed by means of the equation $u = r\omega$, after several transformations is obtained

$$\frac{dc_{u2}}{dr} = \omega - \frac{\dfrac{c_{u2}^2}{r} + \dfrac{a_1\,\omega\,\sin^2\alpha_1}{r\cos^2\alpha_1} - r\,\omega^2}{(1 + \tan^2\beta_2)(c_{u2} - r\,\omega)} \qquad (44)$$

This is the definitive equation for the determination of the whirl component c_{u2} of the outflow velocity. It is a nonlinear differential equation of the first order, whose general solution cannot be obtained because of its complex construction. The most suitable method of solving it is by isoclinical lines. Using this method, the numerical calculations for a turbine stage with nontwisted stator blades of 45° exit angle were undertaken. The axial velocities at the inner radius c_{m1i} and c_{m2i} are again set equal to 1. The rotor speed is so selected that there is equal pressure before and behind the foot of the rotor blades. Furthermore, the exit angle of the nontwisted rotor blades is of such magnitude that the outflow at the foot of the blades is entirely axial. The results of the calculations are shown in figure 16 by the solid lines.

Although the graphic solution of differential equation (44) offers no particular difficulties, engineering practice nevertheless considers it undesirable. It will therefore be best to look for a means of simplifying the calculation. For the greater number of practical cases, such a means is found in the fact that great effort will always be made to obtain outflow as nearly axial as possible throughout the length of the blades in order to keep outflow losses small. If the whirl components c_{u2} of the outflow velocity are small, then the radial-pressure increases will also be small. The radial-pressure increase corresponding to the relations in figure 16 is shown in figure 2 by the dashed line. It must be admitted that, particularly for smaller radius ratios, it is quite small as compared to the radial pressure increase behind the stator. Therefore, investigation of whether a reliable simplification of the calculation

can be obtained by ignoring the pressure differences along the length of blade may be made. The stage drop H is then uniform along the radius r constant. By substituting in equation (30) only the value for the relative inflow velocity w_1 from equation (32), and then substituting in equation (31) the value for the rotor drop, the drop over the whole stage H is obtained

$$H = \frac{1}{2g} w_2^2 - \frac{1}{2g} u^2 + \frac{1}{g} c_{u1} u \tag{45}$$

Further, from the outflow-vector diagram

$$w_2 = \frac{c_{m2}}{\sin \beta_2} \tag{46}$$

By insertion of this in equation (45) an equation for calculating the axial component of the outflow velocity is obtained

$$\frac{c_{m2}^2}{2 g \sin^2 \beta_2} = H + \frac{1}{2g} r^2 \omega^2 - a_1 \omega r \sin^2 \alpha_1 \tag{47}$$

as the outflow angle β_2 is determined by the form of the rotor blade, from this equation the velocity c_{m2} may be calculated. From the outflow-vector diagram is then obtained the peripheral component

$$c_{u2} = r \omega - \frac{c_{m2}}{\tan \beta_2} \tag{48}$$

The velocities so calculated are shown by the dashed lines in figure 16. In the lower portions of the figure are the corresponding degrees of reaction R and the value of the work output h_n, which is now obtained from the equation

$$h_n = \frac{u}{g} (c_{u1} - c_{u2}) \tag{49}$$

As practical cases will not involve going much beyond a radius ratio $r/r_1 = 2$, the results obtained by equations (47) and (48) may be regarded as sufficiently close approximations.

It is observed from figure 16 that with nontwisted blades the axial outflow velocity c_{m2} increases but slowly with increasing radius r. The deflection of the flow toward the axis behind the stator has thus now been reversed to a large extent. The degree of reaction R again reaches 0.5 at a radius ratio of $r/r_1 = 1.9$; on the other hand, the

work output decreases with increasing radius slowly at first and then very sharply. At a radius ratio of $r/r_1 = 2.4$, the work output is already zero. If the blades are made still longer, the parts of the blades beyond a radius ratio of 2.4 will operate as a blower, that is, they will add energy to the flow. Practically, of course, a blading of such height is out of the question. The work output may be made more uniform along the blade length if the radius at which entire axial outflow is obtained is located not at the foot of the blading but further outwards. This can be seen from figure 17. Here the solid lines repeat the data of figure 16 and the dashed lines give the values for a second rotor speed so chosen that the entire axial outflow occurs at a radius ratio $r/r_1 = 1.5$. It is observed that the relations thus obtained are more favorable. The axial outflow velocity c_{m2} is more uniform throughout the blade length and the work output h_n also falls less sharply with increase of radius r. In figure 18 the corresponding results are given for a stator with an outflow angle of 30°. The phenomena already desribed for the 45° stator occur here in still greater degree. In figures 19 and 20 the velocity-vector diagrams are also shown, namely, in the upper rows for the rotor speed giving axial outflow at the foot of the blading and in the lower rows for the speed giving axial outflow at $r/r_1 = 1.5$. The velocity-vector diagrams are shown in the form customary for water turbines. This form is considered clearer than that customary for steam turbines. Figures 21 and 22 show the course of the flow lines for the two outflow angles, respectively. The flow lines in the plane between stator and rotor and behind the rotor are determined by the calculated axial speeds c_{m1} and c_{m2}. The course of the flow lines between these planes is estimated. The figures show quite clearly the deflection of the flow by the stator, which has been frequently mentioned above. With nontwisted rotor blades this deflection is reversed in the rotor. But it must not be concluded from this that flow behind the rotor is once more vortex-free. Figures 17 and 18 show that such is not at all the case. Because of the marked bending of the flow lines in the plane of an axial section, which occurs at small outflow angles α_1 (fig. 22), centrifugal forces are created that possibly extend into the space between the stator and rotor and in that case would counteract the pressure drop in the radial direction. The drop in a radial direction in the stator outflow velocity would thus be diminished and the flow lines straightened. The variation in the relative inflow angles along the rotor blade would be likewise diminished. How far this phenomenon actually occurs remains to be determined experimentally.

3. Practical Calculation of a Turbine Stage

In order to calculate a turbine stage for a certain set of prescribed conditions, it is unnecessary to go back to the equations presented in the foregoing section; instead the calculation may be carried out by making suitable use of the Mollier diagram. If the adiabatic stage drop H_{ad} is prescribed, then the stator drop at the inner radius $h_{ad,i}$ is first selected. A maximum value no greater than will allow the rotor to work at equal pressure at its inner radius ($p_1 = p_2$) will be selected. Of course, on the other hand the rotor may be allowed to operate with some degree of reaction at this point. From the stator drop $h_{ad,i}$, the theoretical stator outflow velocity is determined in the usual manner by means of a velocity scale in the Mollier diagram. The true outflow velocity is obtained by multiplying by the velocity coefficient φ. The variation of exit angle along the blade length is prescribed by the blade form. From the blade angle at the inner radius the whirl velocity component c_{u1i} is obtained. Now the variation of the whirl component for the other radii r also must be calculated. This is done by means of equation (11) for nontwisted stator blades or equation (9) for twisted stator blades. From the variation of the stator outflow angle, the variation of the outflow velocity c_1 is obtained and therewith that of the stator drop h along the blade length. The fact that with large blade spacing the outflow angle of the flow no longer exactly equals the blade-exit angle may be allowed for by an "angle excess." If there is approximately axial outflow from the rotor, then in accordance with what has been said the pressure p_2 behind the rotor blades and consequently the drop H may be regarded as uniform. From the Mollier diagram the adiabatic rotor drop h'_{ad} for each radius is simply taken and from this is obtained by means of equation (3) the theoretical relative rotor outflow velocity $w_{2theoretical}$, and by multiplication with the velocity coefficient φ, the true relative velocity w_2. Now the inflow and outflow velocity-vector diagrams can be drawn and the calculation of the stage completed. The calculation of a second stage to be added to the first cannot, to be sure, be undertaken without further ado in the same manner, because the velocity of inflow into the second stage is no longer purely axial, or entirely uniform throughout the blade length. For not too great lengths of blade these variations, which according to figures 16 to 18 are not very large for nontwisted blades in such a case may probably be ignored, and the calculation may be carried out as for the first stage. In general, however, it must be borne in mind that the vortex current, which is here involved, undergoes changes over greater distances of travel, so that with

larger numbers of stages the prerequisite conditions for the calculation are less well fulfilled. Its reliability for several tandem stages therefore remains to be tested experimentally.

V. SUMMARY

The flow in steam turbines of considerable blade length is strongly affected by the increase in pressure from the axis outward in the space between the stator and rotor. The same phenomenon is observable also in axial superchargers, which make use of a large drop in one stage and hence operate with a pronounced spiral flow. In order to obtain high efficiency in such machines, this phenomenon must therefore be considered in the design of the blades. Its calculation for nontwisted and arbitrarily twisted blades has therefore been given. The flow behind the stator is first considered, the assumptions of closely spaced blades and negligible friction in the gas being made. Thereafter experiments on a stator are reported, which show that the methods of calculation so obtained also reflect very well the actual conditions in a gas subject to friction. Then the calculations are completed for the course of the flow behind the stator. The results are shown in figures 13 to 18 for nontwisted stator blades with exit angles of 30° and 45° and for nontwisted and twisted rotor blades. The degree of reaction varies considerably over the blade depth due to the radial increase of pressure. With a stator blading of 30° exit angle, a rotor blade operates with 50 percent reaction at its outer end when equal pressure exists at its foot and when the blade length is 0.6 of the inner radius. The flow through the stage is first deflected toward the axis in the stator with nontwisted blades. This phenomenon is reversed in the rotor and indeed somewhat overcompensated, if the rotor blades are also nontwisted.

Translation by Edward S. Shafer,
National Advisory Committee
for Aeronautics.

REFERENCES

1. Stodola, A.: Die Dampfturbinen. Julius Springer (Berlin), 4. Aufl., 1910.

2. Darrieus, G.: Contribution au Tracé des aubes radiales des Turbines. Festschrift Prof. Dr. A. Stodola zum 70. Geburtstag, Orell Füßli Verlag, Zürich und Leipzig, 1929, pp. 92-95.

3. Hartmann, W.: Ausfluss- und Kraftmessungen an der Bechauflung einer einstufigen Versuchsturbine im Luftversuchsstand. VDI—Forschungsheft 397, Bd. 10, July/Aug. 1939, pp. 1-20. (British R.T.P. Trans. No. 2393, Ministry Aircraft Prod.)

4. Legally, M.: Ideale Flüssigkeiten. Bd. VII, Kap. 1 of Handbuch d. Phys., H. Geiger u. K. Scheel, ed., Julius Springer (Berlin), 1927, p. 18.

5. Föttinger, H.: Jahrb. d. D. Schiffbautechn. Ges. Bd. 19, 1918, pp. 385, 472.

6. Betz, A.: Göttinger Nachrichten, Bd. 1919, pp. 193, 217.

7. Eck, Bruno: Technische Strömungslehre. Julius Springer (Berlin), 1941, p. 236. (Reprinted by Edwards Bros., Inc. (Ann Arbor), 1944.)

8. Hartmann, W.: Versuche an Einer Dampfturbinenstufe. Archiv für Wärmewirtschaft, Bd. 22, Nr. 4, April 1941, pp. 87-89.

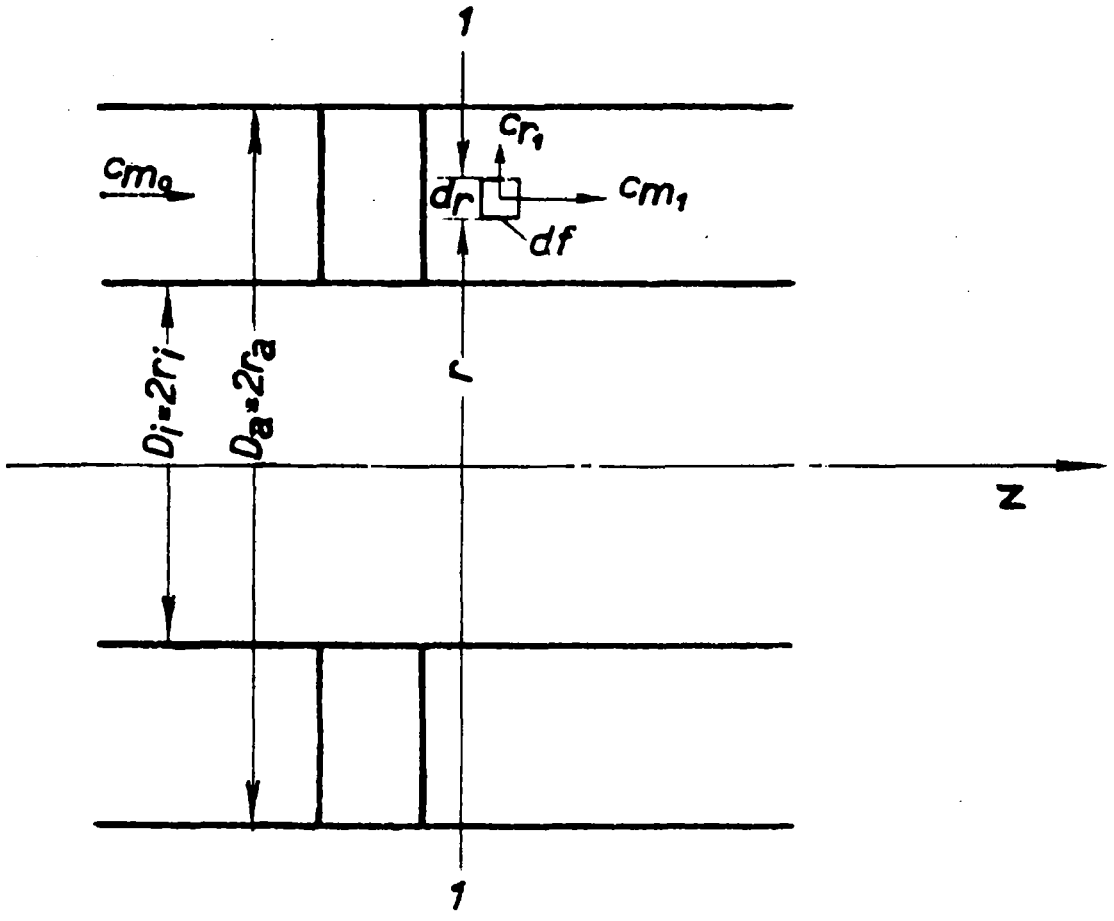

Figure 1. - Flow through a stator.

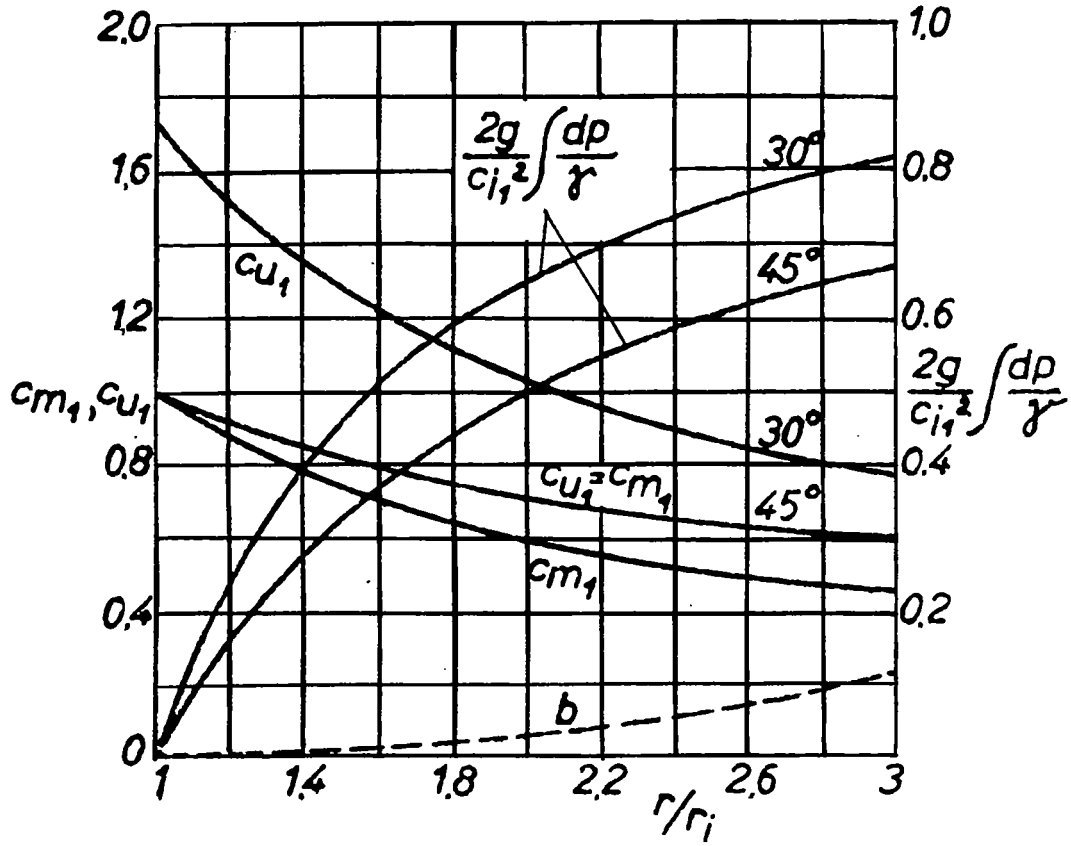

Figure 2. - Graph of velocity components and pressure behind a stator with nontwisted blades of 30° and 45° exit angles.

c_{u1} whirl component

c_{m1} axial component

of c_1, the outflow velocity

c_{1i} outflow velocity at inner radius r_i

dp differential pressure increase

γ specific weight

g acceleration of gravity

r_i inner radius of blading

The dashed curve b shows the variation of pressure behind the rotor according to figure 14.

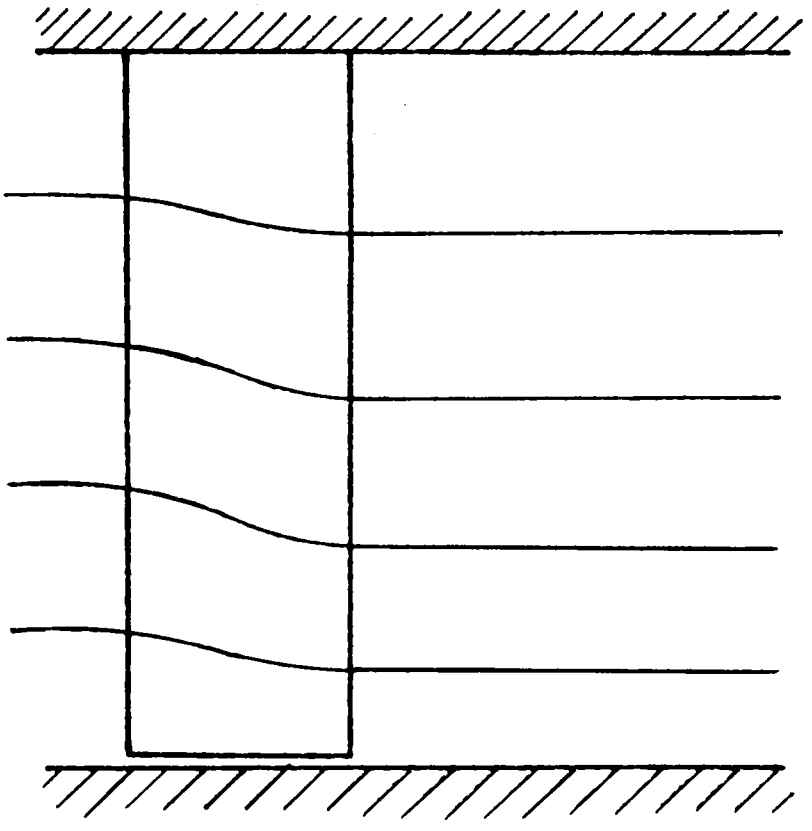

Figure 3. - Course of flow lines through a stator with non-twisted blades of 30° exit angle.

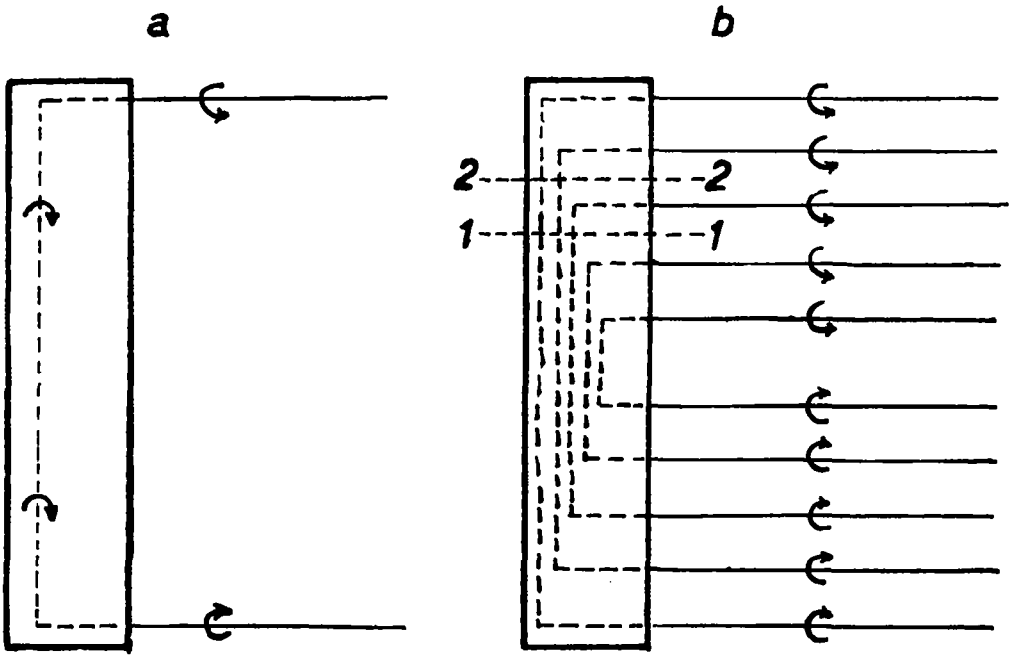

Figure 4. - Replacement of an airfoil of finite span by vortex filaments.

Figure 5. - Photograph of the vortex filaments behind an airfoil of finite span in a water channel.

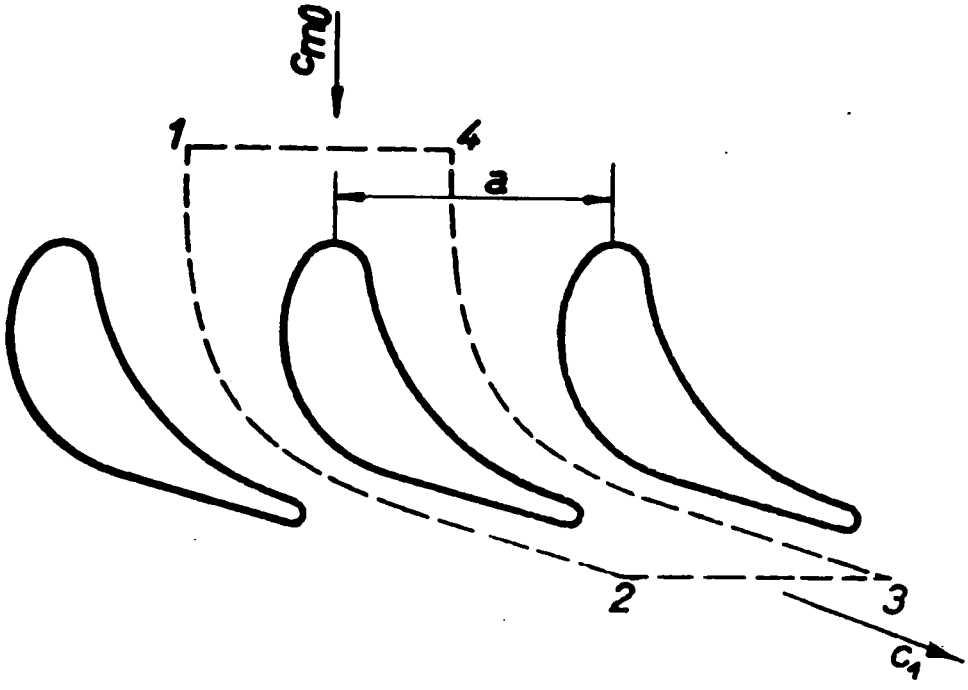

Figure 6. - Stator blading.

Fig. 7

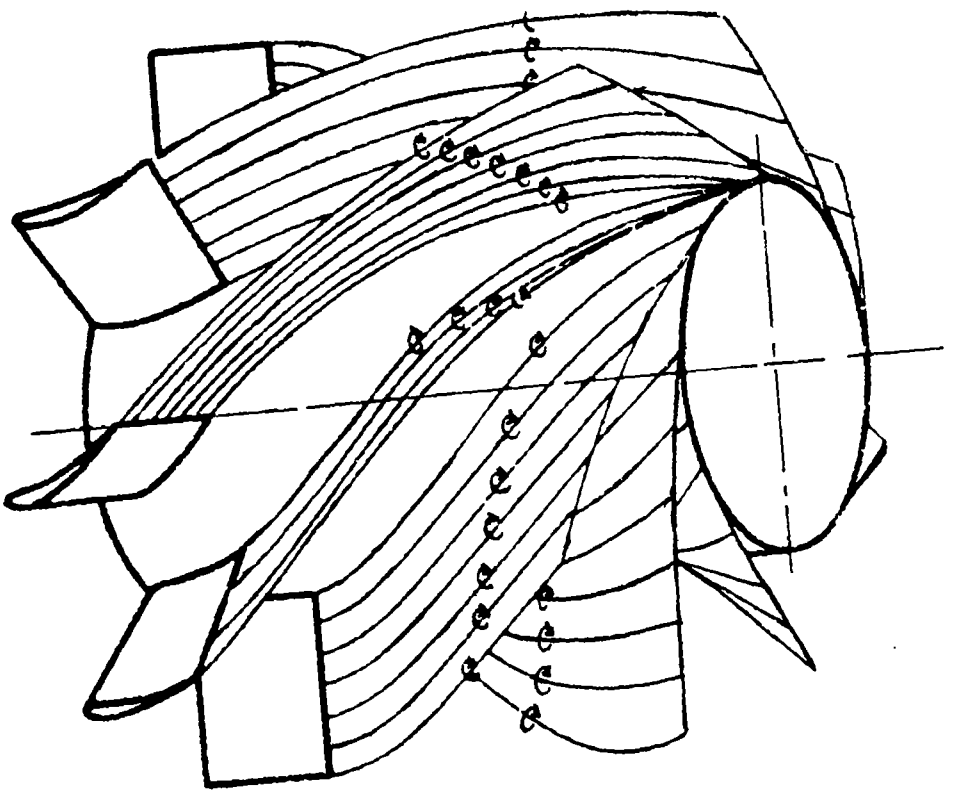

Figure 7. - Vortex filaments behind a stator.

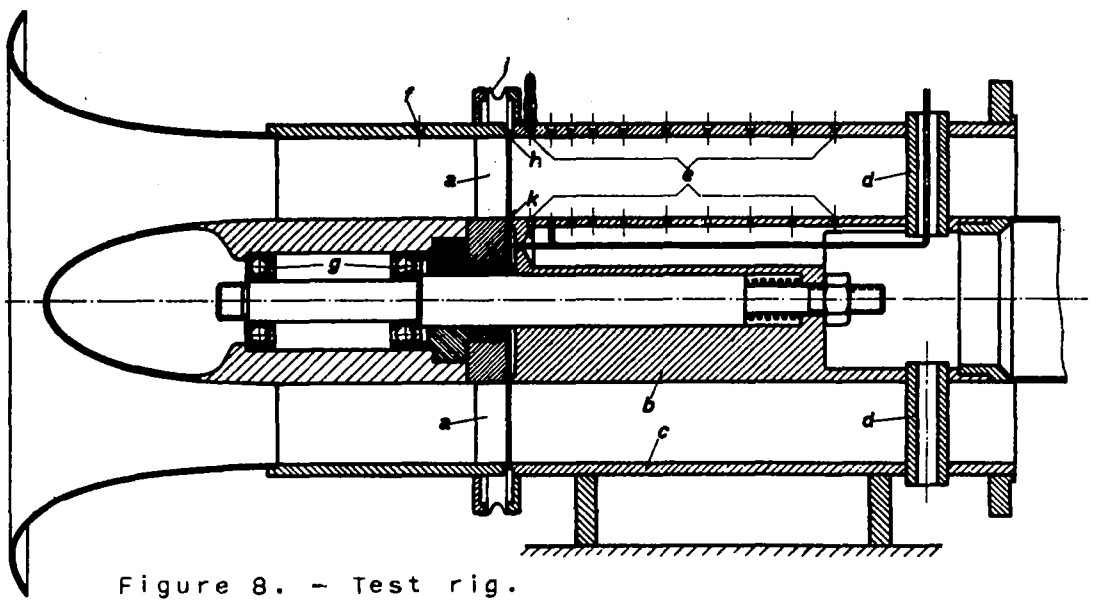

Figure 8. – Test rig.

a. stator
b. inner tube
c. outer tube
e, f. holes for pressure measurements
g. ball bearings
h. outer break in tube wall behind stator
i. rubber membrane
k. inner break in tube wall behind stator

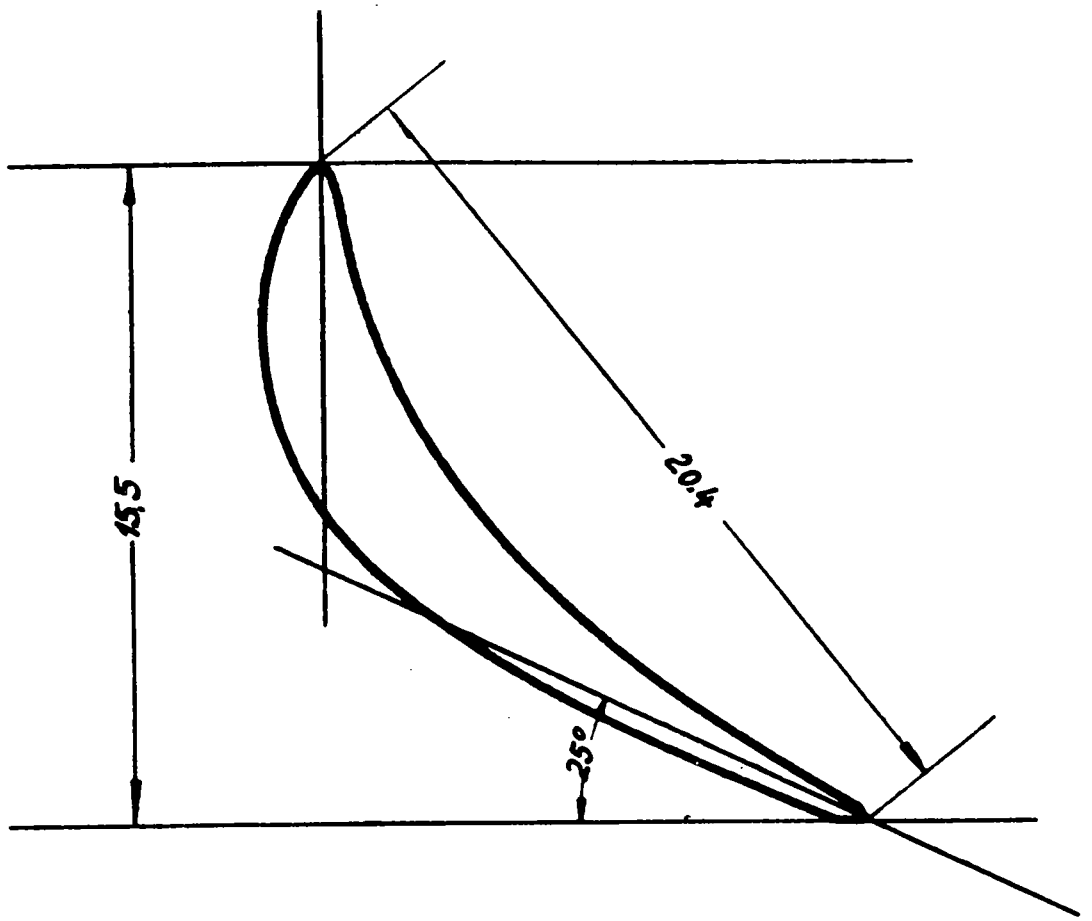

Figure 9. - Blade section used.

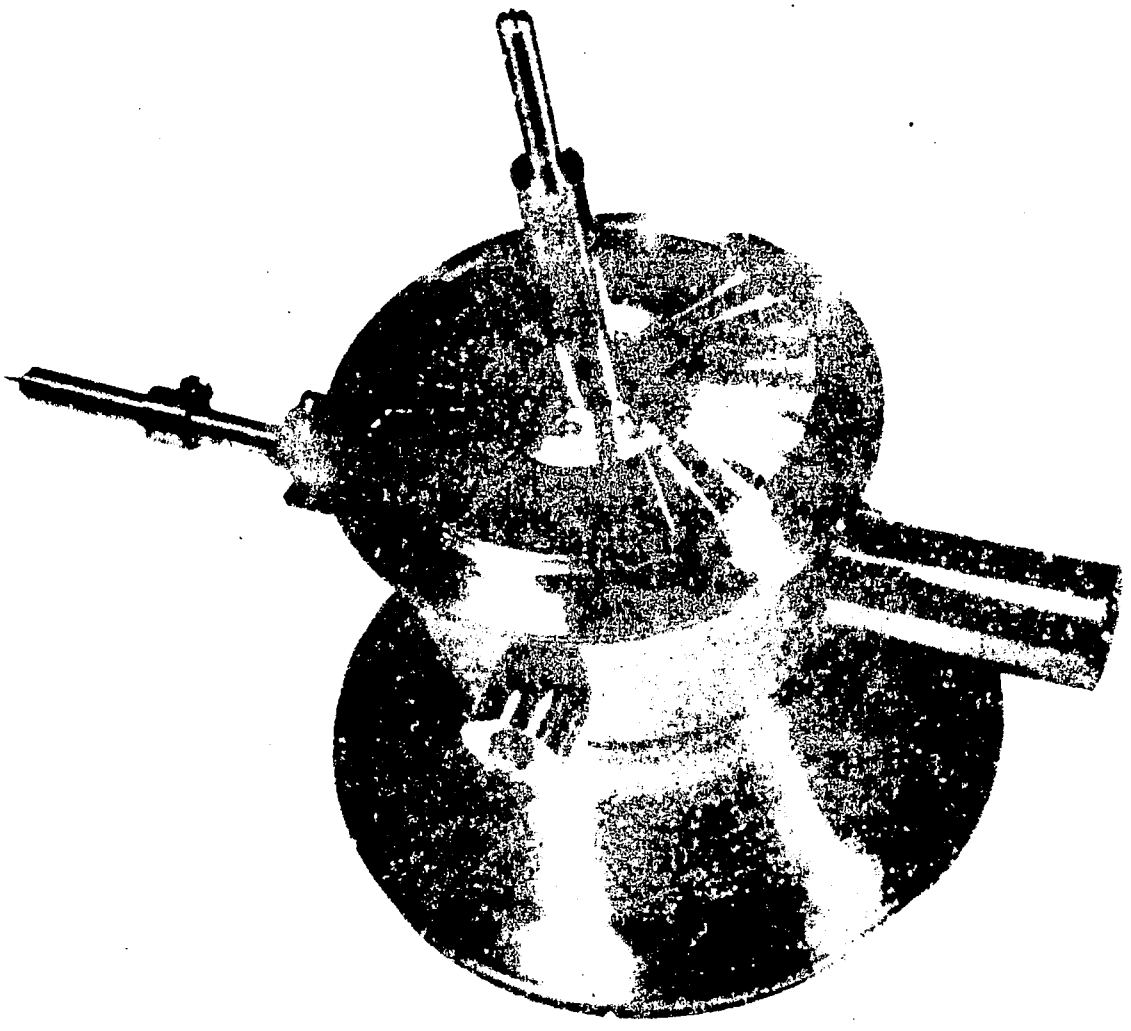

Figure 10. – Forward revolvable part of test rig with stator.

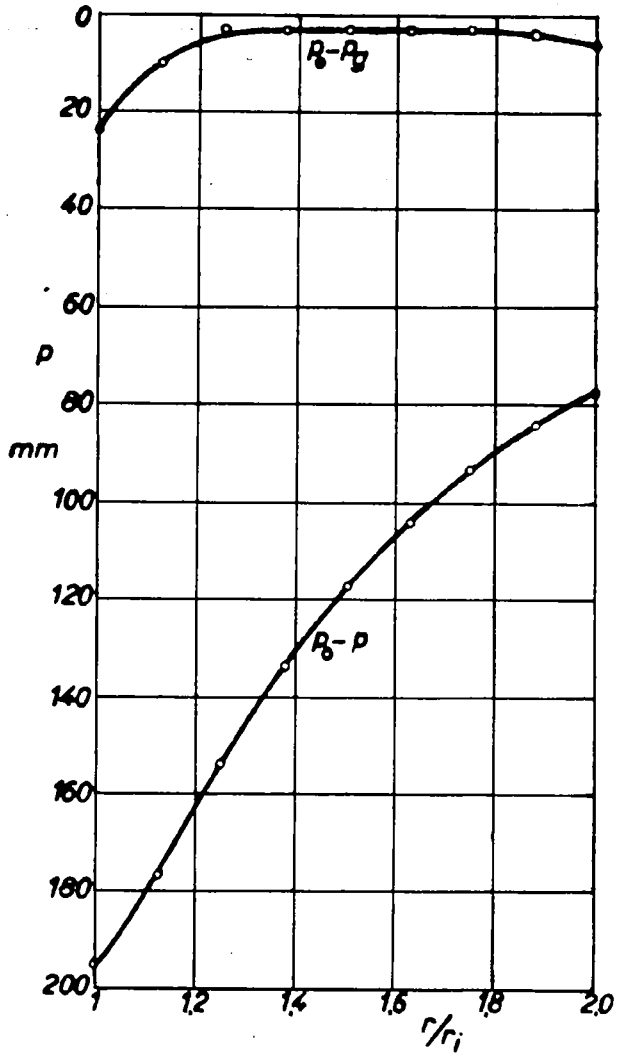

Figure 11. - Measured range of total pressure p_g and of static pressure p at distance r from axis, 25 millimeters behind the stator. The pressures are given in millimeters of alcohol (γ = 813 kg/m^3).

p_0 pressure in the room

r_i inner radius

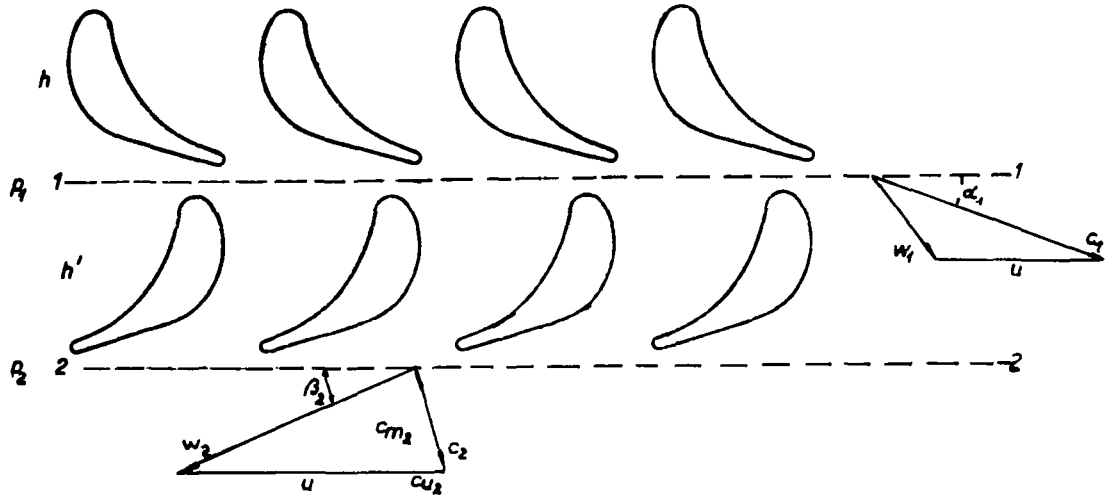

Figure 12. - Stator and rotor of a turbine stage.

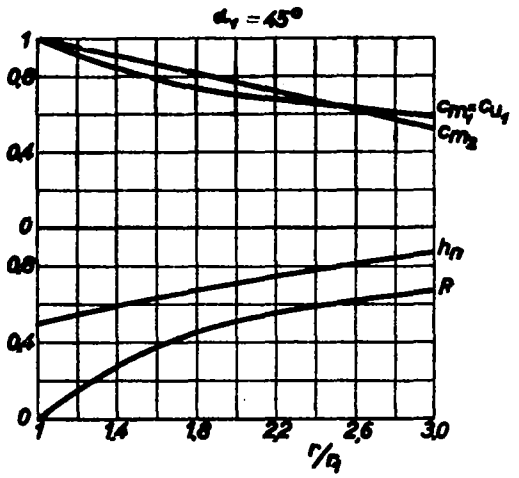

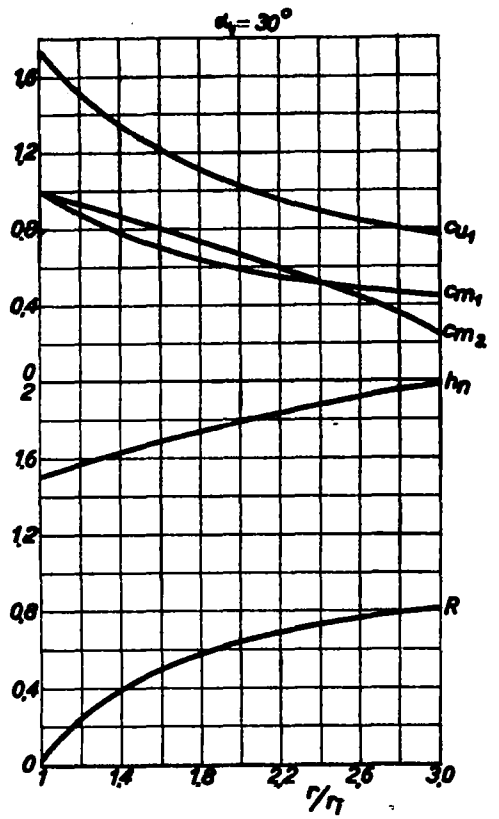

Figures 13 and 14. - Graph of velocity components c_u and c_m, degree of reaction R, and work output h_n over blade length of a turbine stage with nontwisted stator blades having exit angles of 30° and 45° and twisted rotor blades giving strictly axial outflow from the rotor. Pressure is equalized at foot of rotor blades; axial velocity at that point is equal in front of and behind rotor blades.

c_1 outflow velocity from stator

c_2 outflow velocity from rotor

r_i inner radius

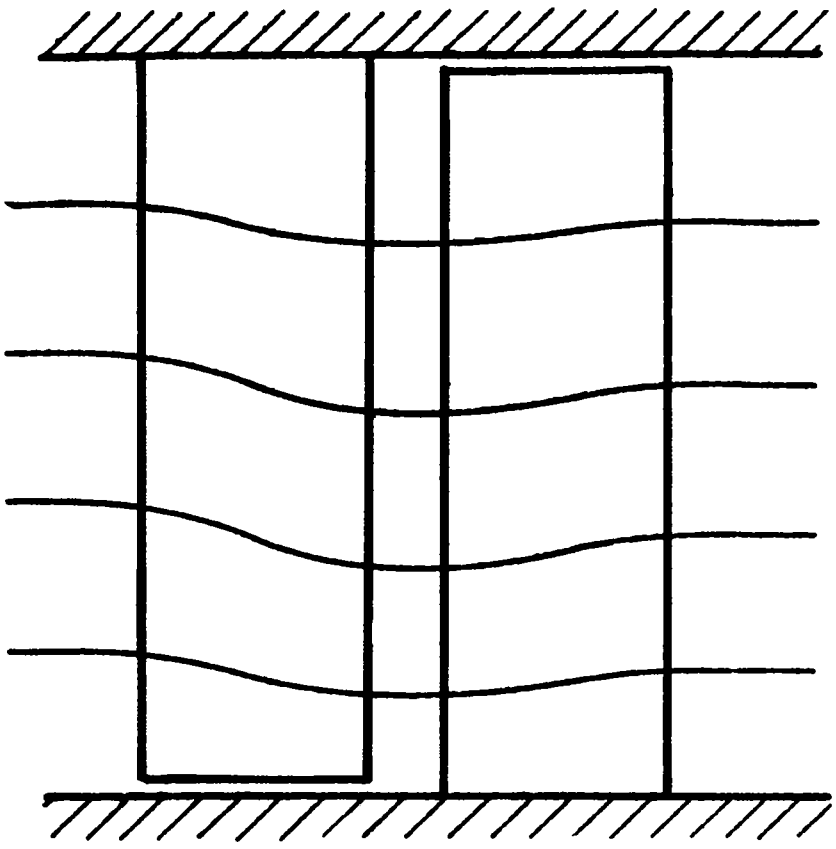

Figure 15. - Course of flow lines through a turbine stage with nontwisted stator blades of 30° exit angle and twisted rotor blades.

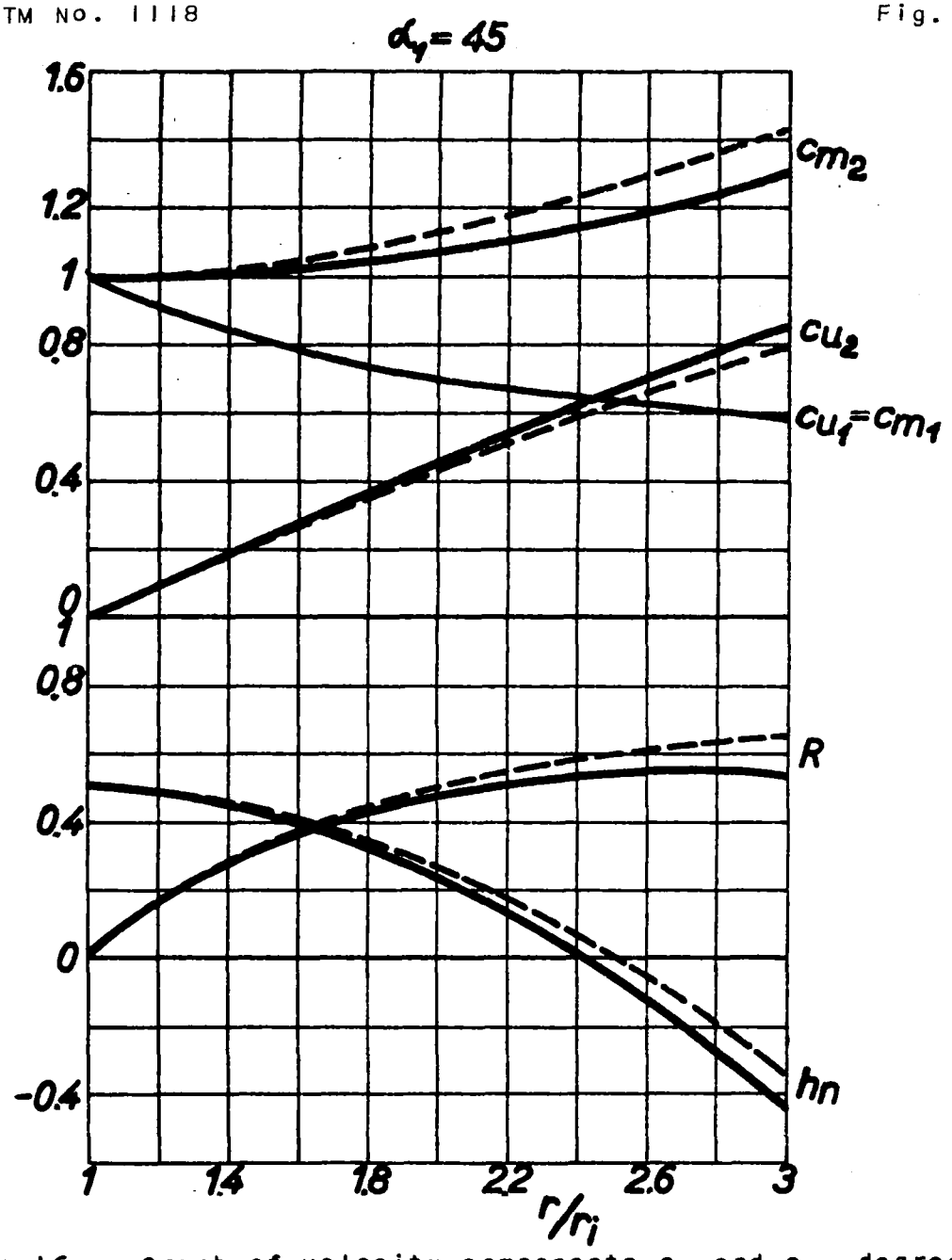

Figure 16. - Graph of velocity components c_m and c_u, degree of reaction R, and work output h_n in a turbine stage having nontwisted stator and rotor blades and fully axial outflow at inner radius r_i

c_1 outflow velocity from stator

c_2 outflow velocity from rotor

——— exact calculation

- - - - approximate calculation

Equal pressure and axial velocity before and behind foot of rotor blades.

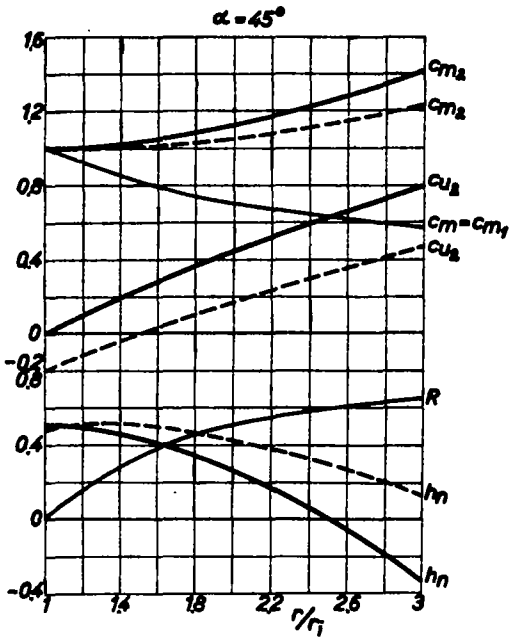

Bild 17.

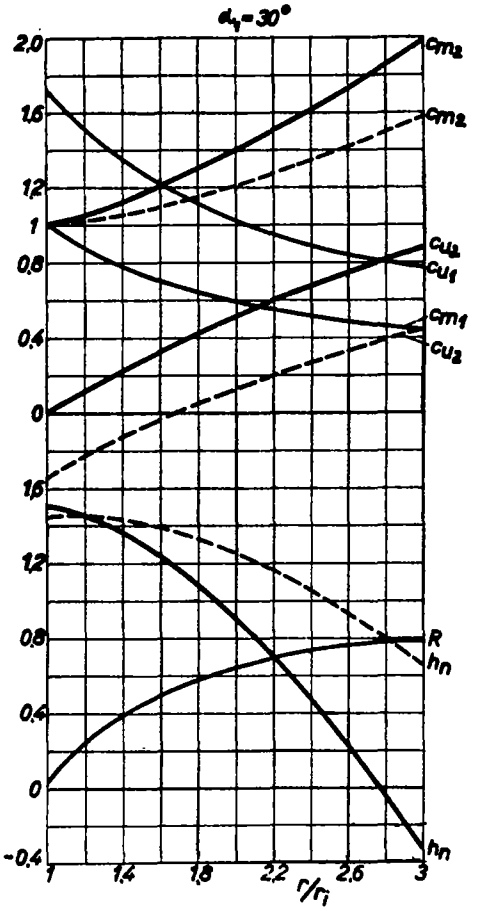

Figures 17 and 18. - Graph of velocity components c_u and c_m, degree of reaction R, and work output h_n of turbine stage with nontwisted blades.

c_1 outflow velocity from stator

c_2 outflow velocity from rotor

——— axial outflow from rotor at inner radius r_i

– – – – axial outflow from rotor at radius $r = 1.5\ r_i$

Equal pressure before and behind foot of rotor blades.

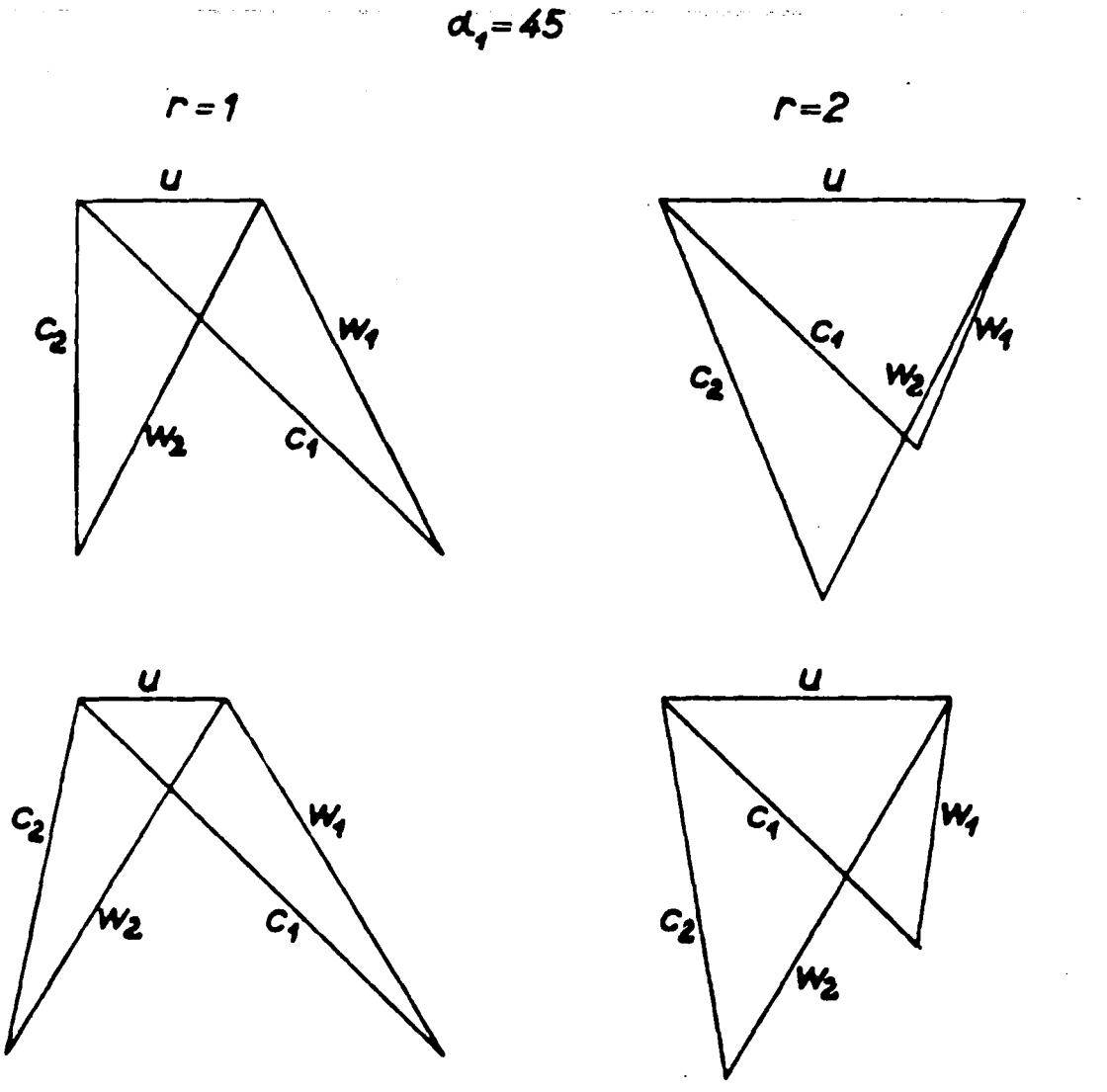

Figure 19. - Velocity-vector diagrams for turbine stage according to figure 17. Above, axial outflow at inner radius r_i; below, axial outflow at radius $r = 1.5\ r_i$.

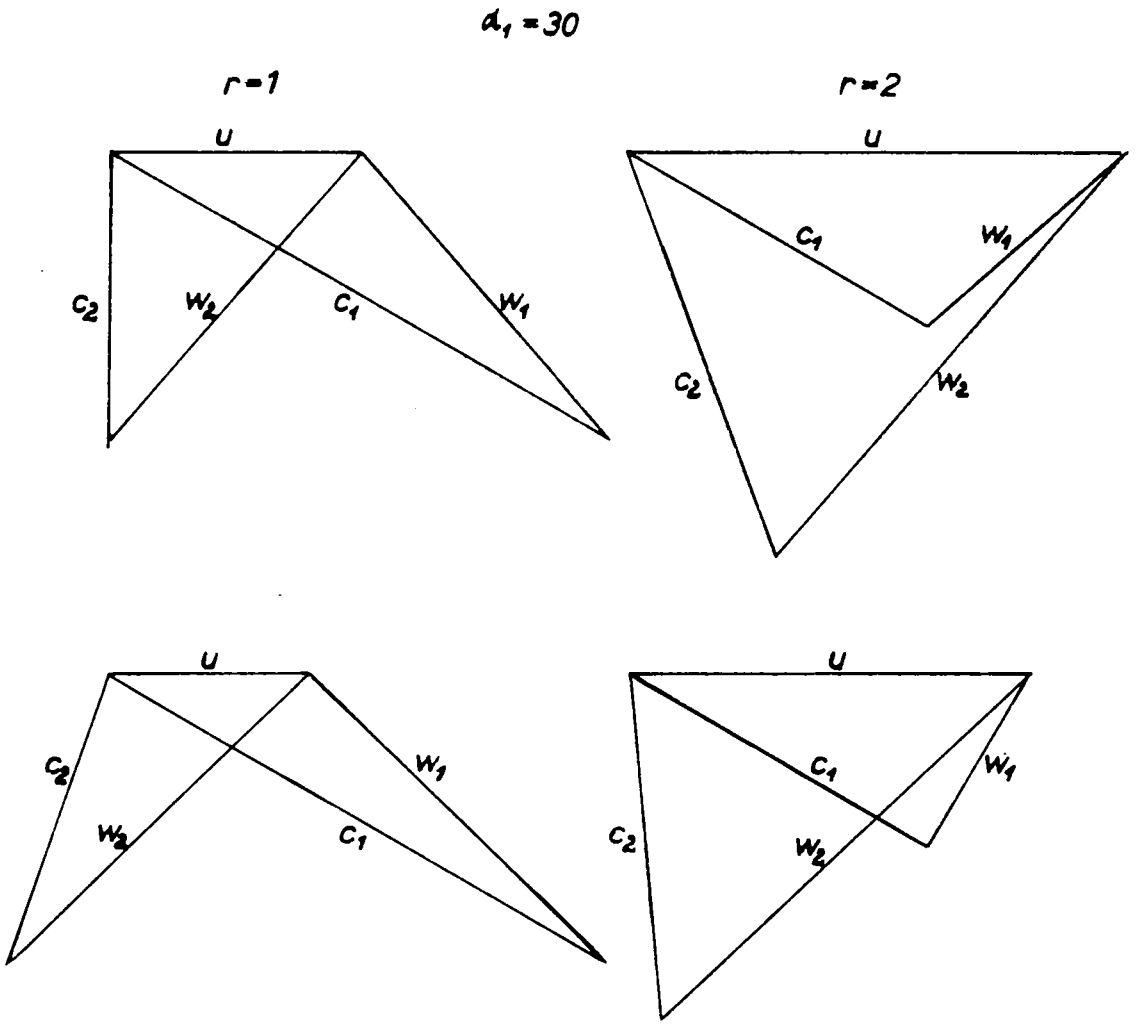

Figure 20. - Velocity-vector diagrams for turbine stage according to figure 18. Above, axial outflow at inner radius r_i; below, axial outflow at radius $r = 1.5\ r_i$.

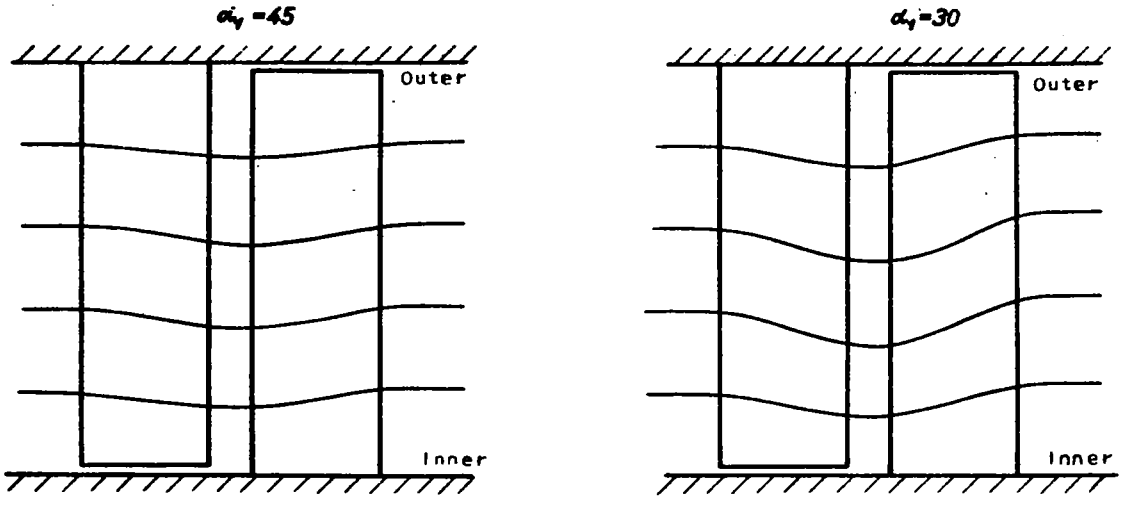

Figures 21 and 22. - Course of flow lines through turbine stage consisting of nontwisted stator blades with exit angles of 30° and 45° and nontwisted rotor blades.